Comparison of Enzyme Polarization of Ligands and Charge-Transfer Effects for Dihydrofolate Reductase Using Point-Charge Embedded *Ab Initio* Quantum Mechanical and Linear-Scaling Semiempirical Quantum Mechanical Methods

STEPHEN P. GREATBANKS,[1] JILL E. GREADY,[1] AJAY C. LIMAYE,[2] ALISTAIR P. RENDELL[2]

[1]*Computational Molecular Biology and Drug Design Group, John Curtin School of Medical Research, Australian National University, PO Box 334, Canberra, ACT 2601, Australia*
[2]*Supercomputing Facility, Australian National University, Canberra, Australia*

Received 28 October 1999; accepted 14 February 2000

ABSTRACT: Using quantum mechanical (QM) methods, we investigated the dependence of a number of factors on the polarization by the enzyme dihydrofolate reductase (DHFR) of its ligands—the substrates, folate and dihydrofolate, and the cofactor NADPH—and evaluated the implications for facilitation of the enzymic reductions. Two quite different levels of QM description of the biomolecular system were used. State-of-the-art *ab initio* QM calculations of the ligands were performed with the bulk DHFR environment modeled using atom-centered point charges. At the other extreme, semiempirical AM1 QM calculations using the linear-scaling Mozyme formalism incorporated in MOPAC2000 allowed for consistent treatment of the 3000-atom system of both enzyme and bound ligands. The study considered the effects of a number of factors on the polarization, including: (i) different levels of *ab initio* QM treatment (HF, MP2, DFT) and basis sets; (ii) different sets of molecular mechanics (MM) point charges in representing the bulk enzyme; (iii) inclusion of the bulk enzyme environment as either point charges in the *ab initio* calculations, or explicitly in

Correspondence to: J. E. Gready; e-mail: Jill.Gready@anu.edu.au

Contract/grant sponsors: ANUSF-Fujitsu Japan Area 3 Agreement; ANU Strategic Development Grant

the semiempirical calculations; (iv) *ab initio* QM calculations of substrate and ligand together (combined system) or separately (noncombined system); (v) degree of charge transfer between substrate and cofactor, and, for the semiempirical calculations, between bound ligands and enzyme; (vi) polarization of the enzyme in the semiempirical calculations; (vii) differences in the behavior of folate and dihydrofolate; and (viii) DHFRs from different species (*E. coli* and human) and different X-ray structure coordinate sets from the same species. Polarization was analyzed mainly by differences in point-charge distributions between gas-phase and bound ligands at the level of complete ligands, subcomponents of ligands (residues), and individual atoms in the pterin and nicotinamide rings involved in the DHFR reactions, but some electron density differences were also calculated. Consistent with our preliminary study (Greatbanks et al., *Proteins* 1999, 37, 157), and earlier work by Bajorath et al. (*Proteins* 1991, 9, 217; 11, 263) for noncombined ligand systems, the DFT calculations showed an unrealistically large dipolar character for individual ligands compared with HF and MP2 results and anomalously large charge transfer to folate from NADPH in combined calculations, which were not shown by the HF or AM1 results. The origin of this behavior is in the representation of the gas-phase anions (the substrates are dianionic and NADPH is tetraanioinic), with the point-charge enzyme-embedded calculations showing polarization similar to the HF results. The analysis highlights that successful modeling of the polarization properties depends on accurate representation of both the gas-phase and enzyme-bound electronic structures of the QM region. For both folate and dihydrofolate at the HF and MP2 levels, changes in density from enzyme binding in the region of the reducible bonds (N8—C7 for folate, C6—N5 for dihydrofolate) is small, with the bulk of the polarization taking place in the N2—C2—N3 region near the Asp27 (or Glu30) active-site group. Polarization at C7 for folate and C6 for dihydrofolate is negative (i.e., does not favor hydride-ion transfer), whereas the trend at N8 for folate, but not at N5 for dihydrofolate, favors protonation. For the Mozyme results, the substrate pterin-ring polarization trends are similar, and also with negligible charge transfer to NADPH, and only a very small charge transfer to the enzyme. For NADPH, the HF, MP2, and Mozyme results indicate charge polarization on binding to the enzyme at the active carbon (C4) of the nicotinamide ring is favorable for hydride-ion transfer (i.e., slightly more negative), with the active hydrogen (H4) also being more negative for the HF and MP2 results. For all methodologies, the nonactive hydrogen (H4′) becomes significantly more positive, which would reduce its potential for transfer. The Mozyme results show a net loss to the enzyme of ~0.3 electrons, mostly from NADPH, which is strongly localized in the vicinity of the substrate glutamate and NADPH diphosphate and 3′-phosphate groups.
 J Comput Chem 21: 788–811, 2000

Keywords: enzyme mechanism; substrate polarization; dihydrofolate reductase; NADPH; electron density differences; linear-scaling quantum mechanics (QM)

Introduction

Understanding the influence of the active-site environment of enzymes on the energetics of the binding of substrates and on the mechanism of the reaction are essential for understanding how they perform their catalytic functions. Of key interest is how the reaction details differ from those in solution, and particularly the features of the enzyme environment that contribute most to facilitation of the reaction. Computational methods in combination with X-ray crystal structures of enzyme complexes represent an increasingly powerful tool for investigating these issues, as they provide the potential for identifying the specific enzyme features, such as particular side-chain groups, whole-enzyme electrostatics, or desolvation effects, which contribute most energetically to the catalysis.[1–3] However, as reactions catalyzed by enzymes vary widely, we can expect that the enzyme designs

evolved for their catalysis will also differ widely and, consequently, that the balance of the catalytically important contributions will also vary. Thus, we require computational methods that can determine this balance, but unfortunately at present there is no one method that can treat all relevant effects with comparable accuracy.

Consequently, a number of hybrid quantum mechanical/molecular mechanical (QM/MM) treatments have been developed (applicable also to nonenzyme condensed-phase systems), which divide the molecular system into QM and MM components, with the former including a minimal fragment of the reacting species necessary for describing the chemistry, and the latter including the rest of the system, including solvent.[4, 5] Such methods vary greatly in the quality of the descriptions of component systems.[6] Most QM/MM studies to date that include a full-protein force-field MM description have been restricted to a semiempirical QM description,[7–10] especially those within an MD simulation to generate free energies and not merely enthalpies.[11, 12] Treatments employing *ab initio* QM have been restricted to a more approximate MM description, such as embedded point-charge fields. However, QM/MM studies employing QM potentials parameterized from *ab initio* or valence-bond QM calculations that permit MD simulations to be undertaken have recently been reported.[13, 14]

We have undertaken computational studies of the mechanism of dihydrofolate reductase (DHFR) using a variety of methods, most recently semiempirical QM/MM within a free-energy perturbation (FEP)/MD simulation.[11] DHFR is a ubiquitous enzyme with a primary function of reducing 7,8-dihydrofolate (DHF) to 5,6,7,8-tetrahydrofolate (THF), in the presence of NADPH cofactor.[15, 16] THF is the precursor of the THF cofactors utilized in many reactions, notably in the production of thymidylate required for cellular DNA synthesis, a requirement that underlies the major pharmaceutical interest in DHFR as a target for cytotoxic drugs. In addition to the conversion of DHF to THF, some DHFRs also catalyze the reduction of folate to DHF, although far more slowly (see Fig. 1). The relatively small size of the enzyme, coupled with the inherent pharmaceutical interest, has inspired experimental and computational research of the enzyme structure and mechanism, particularly using crystallographic approaches.[17, 18] However, many aspects of the mechanism remain unclear.[16]

Most investigations of the mechanism have focused on the origin of the proton required for both

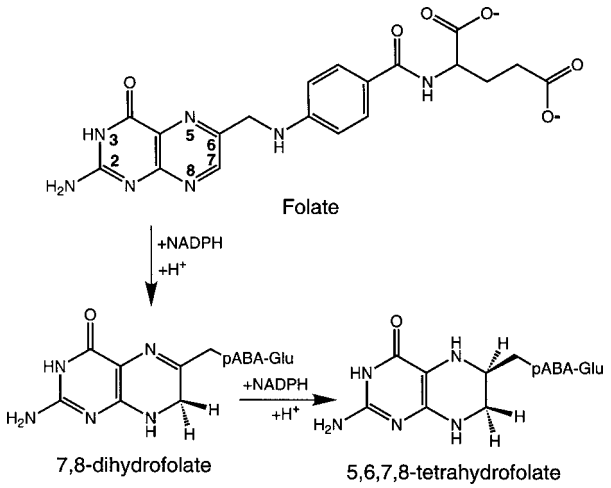

FIGURE 1. Structures of the natural substrates, folate and dihydrofolate, of DHFR and the overall chemistry of the reductions. *p*ABA-Glu represents the *p*-aminobenzoyl-glutamate side chain. Both reduction steps involve a protonation and a hydride-ion transfer (from NADPH cofactor). The order of the additions has not been determined, but it is generally assumed that the protonation occurs first. The source of the protons has not been established, but direct protonation to either N8 or N5 from a protein group is not possible.

reactions but at different sites (N5 and N8 for DHF and folate reductions, respectively), and on the role of the conserved active-site carboxylate group (Asp in bacterial and Glu in mammalian DHFRs), including enzyme-induced changes in protonation state or tautomerization around N3 and O4 of the pterin ring.[17, 19] The series of studies by Bajorath and coworkers in 1991[20–22] is therefore of interest, as their focus was on investigating the possible effect of polarization on the enzymic activation of one or both substrates, or cofactor. Bajorath et al. used density functional theory (DFT) calculations within the local density approximation (LDA) to investigate (individual) polarization of folate or dihydrofolate substrates, or NADPH cofactor within *E. coli* DHFR as represented by a point-charge field. These calculations, which were state-of-the-art at the time, showed that the enzyme environment causes substantial polarization of the ligands. This was attributed as being due mainly to a pair of triads of positively charged residues at the enzyme surface (Lys32, Arg52, and Arg57 for substrates and Arg44, Lys76, and Arg98 for NADPH) causing an effectively dipolar shift of electron density from the pterin ring to the glutamate group at a distance of 18 Å from the substrates, and from the nicotinamide ring to the diphosphate and adenophos-

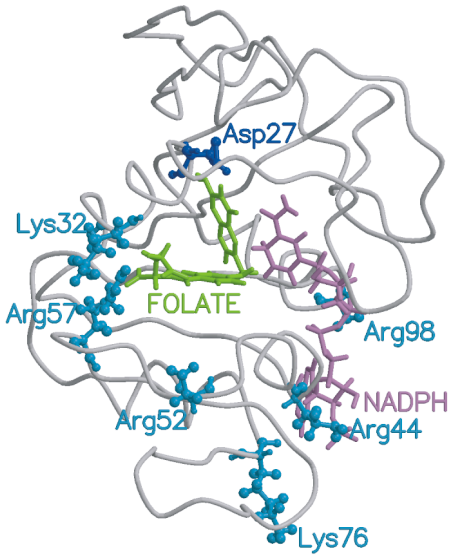

FIGURE 2. Structure of *E. coli* DHFR (PDB code 7DFR) showing the protein backbone, the relative positions of the folate substrate, and the NADPH cofactor. Also shown are the Asp27 residue involved in hydrogen bonding to the N3H and $N2H_2$ groups of the pyrimidine ring of folate and the two triads of charged amino acid residues at the entrances to the folate (Lys32, Arg57, Arg52) and NADPH (Arg44, Lys76, Arg98) binding pockets, respectively. Figure composed using MOLSCRIPT.[24]

phate groups of cofactor, up to 20 Å away. The relative positions of folate, NADPH, and the two charged triads are depicted in Figure 2.

Accurate representation of polarization requires a high-level QM treatment which, as noted earlier, places limitations on the level of MM description that can be used. In the current work, we use state-of-the-art QM calculations within a charge-field embedded-enzyme approximation to investigate a number of factors that may influence the polarization of substrates and cofactor in the enzymic environment. In particular, we evaluate the effects of different types and levels of theoretical treatment. Computational advances since 1991 mean that Hartree–Fock (HF) and more accurate second-order Moller–Plesset perturbation theory (MP2) calculations, including realistic basis sets (sufficiently large to represent electronic polarization effects reasonably), on systems this size are now tractable, although still at the limits of what is currently feasible. As both MP2 and DFT methods allow the effects of electronic correlation to be incorporated in the calculations, we now have, with MP2, access to an alternative correlated method to compare with the results of DFT calculations, as well as the newer gradient-corrected (GGA) DFT methods. In recent preliminary work,[23] we found significant differences in the polarizations of the pterin ring of folate and dihydrofolate using MP2 and DFT methods, with the latter results (including those for GGA DFT methods) showing the same large polarization as that found by Bajorath et al.,[20–22] but with relatively small polarizations shown by MP2 and HF results. The current study extends this work to consider polarization of the cofactor NADPH, as well as study of the combined substrate and cofactor system at the DFT and HF levels.

For these *ab initio* QM calculations, we have modeled the bulk DHFR environment using sets of atom-centered point charges. Such point-charge models are commonly used[25, 26] and correspond to the electrostatic component of more complete QM/MM methods. It should be borne in mind that the dielectric environment within the enzyme will differ from the gas-phase conditions used in the generation of the point-charge values. Although scaled (smaller) point-charge values would provide a more accurate representation, the scaling, necessarily, should be nonuniform and there is no simple way to calculate appropriate scaling. The Mozyme calculations described in what follows implicitly represent the enzyme dielectric. To evaluate contributions of structural and species effects to the polarization, we have considered two *E. coli* DHFR structures[18, 27] (7DFR and 1RA2) as well as a human DHFR structure,[28] 1DRF. Whereas all three structures contain folate, cofactor, in its oxidized $NADP^+$ form, is present only for the *E. coli* structures.

To evaluate the level of agreement of semiempirical QM methods with these high-level QM calculations for predicting the pattern of polarization of ligands by the enzyme, we undertook complementary calculations at the other extreme to the QM/MM model. We performed semiempirical calculations using the recently introduced Mozyme formalism of Stewart,[29] now incorporated in MOPAC2000,[30] which allows the entire enzyme system to be explicitly included in the calculations. In addition to providing a very different level of QM treatment for the comparison of the degree of electronic polarization, charge transfer to the enzyme, not allowed in the *ab initio* point-charge calculations, can be readily investigated using this methodology. Together with the *ab initio* QM calculations, these calculations allow us to determine the nature, extent, and variability of polarization of substrate and cofactor in the reactive enzyme complexes for both folate and dihydrofolate reductions, and to assess whether

such polarization could significantly facilitate the reactions.

Computational Methods

HF AND MP2 QM METHODS

Ab initio QM calculations were mostly performed using a locally tuned version of the GAUSSIAN-94 suite of programs[31] on a Fujitsu VPP300 vector supercomputer at the Australian National University supercomputing facility. However, convergence was very difficult for these large anionic DFT calculations and often failed with GAUSSIAN. In these cases, TURBOMOLE,[32] running on SGI R8000 or 10000 platforms usually converged better because of the automatic damping procedure controlling the oscillations in the SCF. HF, MP2, and DFT calculations were performed using a number of basis sets (3-21G, 6-31G*, 6-31+G*). When possible, calculations using basis sets that include diffuse functions (6-31+G*) known to be required for correct modeling of anionic systems[33] were performed. Some HF and DFT calculations with the even larger 6-31++G* basis set were undertaken in the initial study.[23] The largest calculations at the HF level were for the combined folate and NADPH system with 123 atoms and 1618 basis functions for the 6-31+G* basis set, and at the MP2 level for noncombined NADPH with 74 atoms and 784 basis functions with the 6-31G* basis set. At the DFT level the largest calculations for the 123-atom combined system had 1298 basis functions with the 6-31G* basis. Point charges were incorporated in the Hamiltonians of the calculations to model the polarizing effect of the bulk enzyme, with the calculations performed to self-consistency (changes in the density matrix $<10^{-7}$ for the DFT calculations, $<10^{-8}$ for the HF and MP2 calculations). In all cases, the polarization was determined by considering changes in charge distribution or electron density between the gas-phase and enzyme-embedded calculations.

DFT METHODS

Local density functional (LDA) calculations, originally developed for solid-state physics problems, have been shown to perform relatively well in reproducing properties of metallic systems. However, they perform less well for covalently bonded systems of chemical interest, for which functionals that incorporate terms depending on the gradient of the density have been developed. These gradient-corrected algorithm (GGA) methods are known to reproduce many molecular properties well, often as well as MP2 theory.[34] However, although there is now an extensive body of literature establishing the general success of these methods,[35–37] the ability of GGAs to represent anionic structures accurately has been relatively little tested, and a number of anomalous results and pathologically poorly treated systems, even for small molecules,[36, 38] have been reported. In this study, the LDA and GGA methods used were SVWN5[39, 40] and B3LYP,[41, 42] respectively. The initial study[23] also used the BLYP and BPW91 GGA formalisms, which gave results most similar to the SVWN5 results, with the B3LYP results being most dissimilar.

MOZYME

The Mozyme approach of Stewart[29] is a formulation of semiempirical molecular orbital theory that utilizes localized molecular orbitals, and is specifically designed for enzyme (i.e., protein) systems. The method has now been incorporated into MOPAC2000.[30] The size of the calculation scales approximately linearly with the size of the system, making it possible to perform semiempirical QM calculations in which both the ligands and enzyme are fully and self-consistently included. In this way, the calculations can represent both polarization and charge-transfer effects in a more realistic manner than by using point charges. Although test studies with the Mozyme methodology have demonstrated that geometry optimization of protein systems large enough to be of biochemical interest is feasible[43] we have restricted our studies to single-point calculations to allow for direct comparison with the *ab initio* calculations.

ELECTRONIC DENSITIES AND CHARGES

For the *ab initio* calculations, the polarization due to the enzyme was quantified primarily in terms of changes in the per-atom and summed per-residue charges, using the partitioning scheme suggested by Bajorath et al.[20, 21] for folate and NADPH shown in Figures 3 and 4, respectively. Mulliken charges[44] are reported here only; alternative schemes (e.g., the Merz–Kollman approach) give the same polarization behavior, although the magnitudes of computed per-atom and per-residue charges differ substantially.[23] In all cases, the polarization is given by $\Delta(B - F)$—that is, the difference between the ligand charge distribution while bound to the enzyme (B) and for the free ligand in the gas phase (F). In addition, changes in the electron density [again,

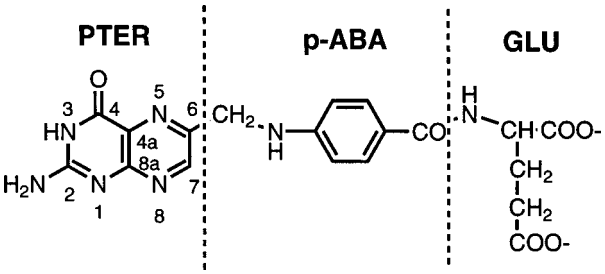

FIGURE 3. Scheme for partitioning the folate substrate into PTER, *p*-ABA, and GLU residues, as used by Bajorath et al.[20] for calculating net charges. PTER is the pterin ring, *p*-ABA is the *N*-methylene-substituted *p*-aminobenzoic acid fragment, and GLU is the glutamate group.

$\Delta(B - F)$] were calculated for selected cases: plots of the polarization isosurfaces at the HF and LDA levels of theory are shown in Figure 5.

For the AM1 Mozyme calculations, the charge polarization of ligands was calculated using default MOPAC charges. Although MOPAC2000 can calculate full Mulliken charges, this option is not implemented in the Mozyme option. However, as for our tests for the *ab initio* cases, the polarization pattern is expected to be insensitive to the choice of charges. For Mozyme calculations that allow polarization of the enzyme on binding of the ligands, the charge polarization of the whole enzyme could be calculated. Such a plot is shown in Figure 7.

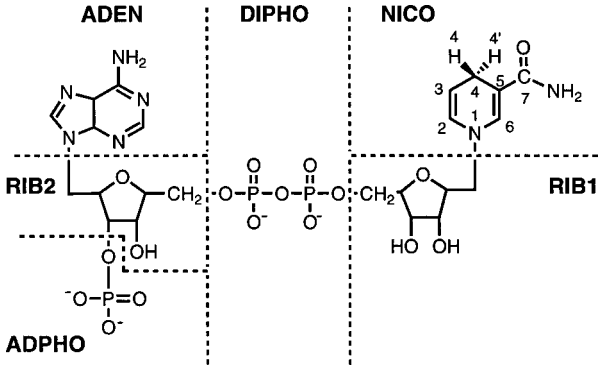

FIGURE 4. Scheme for partitioning the NADPH cofactor into NICO, RIB1, DIPHO, RIB2, ADPHO, and ADEN residues, as used by Bajorath et al.[21] for calculating net charges. NICO is the nicotinamide ring containing the active hydride ion H4 (*pro-R* hydrogen) on C4; ADEN is the adenine ring; RIB1 and RIB2 are the ribose rings attached to NICO and ADEN, respectively; DIPHO is the diphosphate bridge; and ADPHO is the 2′-phosphate group on RIB2.

ENZYME AND LIGAND MODEL GENERATION

Model structures for two different *E. coli* DHFRs were constructed from the Protein Data Bank (PDB) entries 7DFR and 1RA2. In addition, a model of human DHFR was constructed from the 1DRF PDB entry. The 7DFR and 1RA2 structures contain both bound folate and $NADP^+$, from which NADPH can be readily constructed, whereas the 1DRF structure contains bound folate only. To avoid arbitrary effects from model construction and relaxation, we have not modeled NADPH into the human structure. The human DHFR is somewhat larger than that from *E. coli*, having 186 rather than 159 amino acid residues. At neutral pH, the *E. coli* enzyme has a large net charge of −11, whereas human enzyme has zero net charge.

INSIGHTII[45] was used to generate the enzyme models, adding hydrogens at appropriate positions for the required pH, as well as any missing portions of residues. The terminal groups were charged. All systems reported in this article are at pH 7; test calculations at other pH values gave similar results, so this variable was not pursued. All crystallographic water molecules were removed. This action is justified as they provide only a limited representation of the bulk solvent environment, and because our aim is to determine the polarization due to the enzyme environment under a number of different conditions and with different methods.

Heavy-atom positions for the substrate (folate or dihydrofolate) and the cofactor (NADPH) were retained from the X-ray structures and, after addition of hydrogens at appropriate positions, the geometry was allowed to relax using the PM3 Hamiltonian, as implemented in the GAUSSIAN-94 program. This simple protocol, used also in the initial study,[23] retains the overall enzyme-bound conformations of ligands. For purposes of the study (i.e., to calculate polarization by the enzyme using different theoretical methods), a common structure across all methods is desirable.

The resultant QM model structures contain 49 or 51 atoms for folate or dihydrofolate substrates, respectively, and 74 atoms for the NADPH cofactor. For the *ab initio* calculations where the enzyme was represented using point charges, the models included an additional ∼2650 or ∼3000 point charges in the Hamiltonian for *E. coli* and human DHFRs, respectively. The point charges were taken mostly from the AMBER95 force field,[46] but some calculations were done with charges from the CFF91,[47] CVFF,[48] and ESFF[49] force fields as also implemented in the INSIGHTII program. The largest

systems treated using *ab initio* QM methods are the *E. coli* models, which contain both bound folate and cofactor with 123 QM atoms. The semiempirical calculations performed using the Mozyme approach considered the 1DRF human DHFR and 7DFR *E. coli* DHFR structures and included the full enzyme and substrate system and, in addition, the NADPH cofactor for the *E. coli* DHFR system. The largest human DHFR system contained 3064 atoms.

Clearly, there are a number of approximations in the generation of these models. As discussed at greater length in the initial study,[23] these are reasonable for the present purposes of investigating how the general model features, such as DHFR species and use of different theoretical methods, affect the magnitude, direction, and distribution of the ligand polarization. It is necessary to assess the scale and variability of the all-enzyme polarization before making judgments as to whether it might contribute significantly to facilitating the enzymic catalysis and, if so, what specific aspects of the models need to be improved. It is noteworthy that, although the model-generation protocols used here differ substantially from those employed by Bajorath et al.,[20–22] the LDA DFT polarizations we calculated in our initial study are very similar to their results.

Results

The study was designed to evaluate the importance of a number of factors for calculating the polarization of ligands on binding to DHFR, and also charge transfer between ligands and with the enzyme. These factors include the importance of the level of theory (Tables I, IV–IX), basis set (Table I), choice of charges used for representing the enzyme (Table II), and choice of crystal structure coordinates (Table III). The results allow evaluation of the effects of considering substrate and cofactor as a combined QM system for the *ab initio* studies (Tables I and III–V), which allows the possibility of charge transfer between the ligands, compared with individual isolated substrates as done previously.[20–23] The Mozyme results also allow evaluation of charge-transfer effects between the ligands, but also with the protein (Tables VII–IX). Atom-wise comparisons of charge and density polarizations of the pterin

TABLE I.
Polarization[a] for Combined QM System of Folate and NADPH within *E. coli* DHFR (7DFR) at HF and DFT LDA (SVWN5) Levels, for 3-21G, 6-31G*, and 6-31+G* Basis Sets (Some Previous and New Results for Noncombined Systems Are Included for Comparison).

	3-21G		6-31G*		6-31G+G* [c]	Bajorath[d]	6-31G** [e]			
[b]	HF	LDA	HF	LDA	HF	LDA	HF	MP2[f]	LDA	GGA
PTER	0.033	0.538	0.028	0.536	0.058	0.61	0.04	0.04	0.47	0.32
p-ABA	0.059	0.159	0.062	0.158	0.083	0.00	0.06	0.08	0.10	0.10
GLU	−0.097	−0.317	−0.095	−0.316	−0.116	−0.61	−0.10	−0.12	−0.57	−0.42
Total	−0.005	0.380	−0.005	0.378	0.025	0.00	0.00	0.00	0.00	0.00
DIPHO	−0.095	−0.176	−0.102	−0.181	−0.131	−0.24	−0.104	−0.105	−0.162	
RIB1	0.056	0.098	0.059	0.098	−0.090	0.25	0.058	0.060	0.118	
RIB2	0.016	−0.044	0.028	−0.038	0.038	−0.04	0.028	0.025	−0.017	
ADPHO	−0.008	−0.163	−0.013	−0.165	−0.002	−0.44	−0.013	−0.016	−0.167	
ADEN	0.003	−0.219	0.003	−0.219	0.017	−0.04	0.003	0.003	−0.185	
NICO	0.032	0.126	0.031	0.127	0.143	0.51	0.028	0.032	0.412	
Total	0.005	−0.380	0.005	−0.378	−0.025	0.00	0.000	0.000	0.000	

[a] Polarizations in terms of summed per-residue Mulliken charges, totaled for each ligand.
[b] Residue partitioning as in Figures 3 and 4.
[c] DFT calculation failed to converge.
[d] Bajorath et al.[20, 21] calculations with the 6-31G** basis set were performed on folate and NADPH separately.
[e] Noncombined folate with the 6-31G** basis set from ref. 23. The DFT GGA method is B3LYP. Noncombined NADPH for HF, MP2 and LDA from this work.
[f] MP2 NADPH results for 6-31G* basis.

TABLE II.

Per-Residue Charges[a] for Different Point-Charge Representations of *E. coli* DHFR Enzyme (1RA2) for Combined QM System of Folate and NADPH at HF Level with 6-31G* Basis Set.

	Gas phase	AMBER95[b]	CFF91[c]	CVFF[d]	ESFF[e]
PTER	−0.113	−0.055	−0.056	−0.050	−0.056
p-ABA	0.095	0.139	0.140	0.118	0.141
GLU	−2.001	−2.112	−2.111	−2.096	−2.113
Total	−2.019	−2.028	−2.027	−2.028	−2.028
DIPHO	−2.521	−2.553	−2.574	−2.544	−2.580
RIB1	0.574	0.615	0.618	0.608	0.619
RIB2	0.838	0.840	0.858	0.873	0.857
ADPHO	−2.104	−2.146	−2.165	−2.183	−2.159
ADEN	−0.443	−0.431	−0.418	−0.426	−0.422
NICO	−0.325	−0.297	−0.292	−0.302	−0.288
Total	−3.981	−3.972	−3.973	−3.974	−3.973

[a] Charges are summed per-residue Mulliken charges.
[b] Ref. 46.
[c] Ref. 47.
[d] Ref. 48.
[e] Ref. 49.

(*ab initio*: Tables IV and VI, Fig. 5; Mozyme: Tables VII and VIII, Fig. 6) and nicotinamide (*ab initio*: Table V and Fig. 5; Mozyme: Table IX and Fig. 6) rings involved in the reaction, including comparison for folate and dihydrofolate (Tables VI and VII), allow assessment of their possible significance in facilitating the reductions at C6 or C7, or preprotonations at N8 or N5.

HF, MP2, AND DFT POLARIZATION OF SUBSTRATE AND NADPH

For the large combined system comprising both folate and NADPH within *E. coli* DHFR (7DFR), it is evident from Table I that the folate substrate and NADPH cofactor are substantially more polarized at the LDA level than at the HF level, regardless of

TABLE III.

Polarization[a] for Combined QM System of Folate and NADPH (SC) within *E. coli* DHFR (7DFR and 1RA2), and for Folate Only (S) within *E. coli* (7DFR) and Human (1DRF) DHFRs, at HF Level with 6-31G* Basis Set.

	7DFR (SC)	1RA2 (SC)	7DFR (S)	1DRF (S)
PTER	0.028	0.058	0.037	0.041
p-ABA	0.062	0.044	0.059	0.050
GLU	−0.095	−0.111	−0.096	−0.090
Total	−0.005	−0.009	0.000	0.000
DIPHO	−0.102	−0.032	—	—
RIB1	0.059	0.041	—	—
RIB2	0.028	0.002	—	—
ADPHO	−0.013	−0.042	—	—
ADEN	0.003	0.012	—	—
NICO	0.031	0.028	—	—
Total	0.005	0.009	—	—

[a] Polarizations in terms of summed per-residue Mulliken charges, totaled for each ligand.

the basis set used. This is consistent with the previous results of Bajorath et al.[20, 21] showing large polarization at the LDA level, and a selection of our initial results[23] for folate and new results for NADPH for the individual ligands ("noncombined" systems) also shown in Table I. This difference between levels of theory is particularly noticeable for the PTER and GLU groups of folate, and the NICO group of NADPH. Whereas for both HF and MP2 methods, for all basis sets, the effect of the enzyme is to shift electron density from the PTER and *p*-ABA groups toward the GLU group, this effect is very much larger for the LDA method, and is very large irrespective of the LDA method used or the inclusion (Bajorath) or omission (our work) of NADPH in the point-charge system. The same effect was seen for dihydrofolate.[22, 23] Very large polarization of folate was also shown in our earlier work for a series of more accurate GGA density functionals (a B3LYP result is included in Table I). MP2 calculations for the combined substrate and cofactor systems are not reported as these are beyond our computational resources. However, MP2 polarization results for the folate-only QM system (i.e., noncombined system with NADPH not included in QM region) from the initial study (also shown in Table I) and NADPH-only QM system (Tables I and V), as well as folate and DHF results in Table VI, are similar to the HF polarizations.

Although the HF results in Table I for combined and noncombined NADPH (i.e., with and without folate in the QM system) are similar, the LDA results show significant differences that are localized mostly to the NICO group. Also, although the polarization pattern for our noncombined NADPH LDA results correlate well with those of Bajorath et al.,[21] there are differences, particularly for the ADPHO and ADEN groups. These may be due to differences in the model used or a different parameterization of the SVWN functional used in the earlier work of Bajorath et al.[20–22]

POLARIZATION FOR COMBINED QM SYSTEM OF FOLATE AND NADPH

Results for the combined QM system of folate and NADPH given in Tables I–III extend the previous treatment by Bajorath et al. and our initial work by allowing the possibility of mutual polarization and charge transfer between ligands, both in the gas phase and enzyme-embedded states. It is clear from these results that charge transfer at the HF and MP2 levels is minimal for all basis sets, but that charge transfer at the LDA DFT levels is very large with a net transfer of almost 0.4 electron from (dianionic) substrate to (tetraanioic) NADPH.

POLARIZATION OF PTERIN AND NICOTINAMIDE RINGS FROM *AB INITIO* QM

Insights into the effect of the enzyme at the different levels of *ab initio* theory can be deduced by considering changes in the charge distributions within the pterin rings of folate and dihydrofolate substrates and the nicotinamide ring of NADPH as shown in Tables IV–VI. The results in Tables IV and V for combined folate and NADPH within *E. coli* DHFR (7DFR) with the 6-31G* basis set are from the same calculation reported in Table I. For folate at the HF level, the slight increase in negative charge on N8 [−0.017] coupled with the slight decrease in positive charge on C7 [−0.012] suggests that the enzyme environment would more likely promote protonation at N8 rather than direct hydride-ion attack at C7. However, at the DFT level, there is a slight increase in the positive charge at C7 [0.015] while N8 becomes less negative [0.029], but with N8 being very substantially more negative overall than at the HF level. This pattern is the reverse of the HF result, and suggests that the enzyme environment would slightly promote hydride-ion attack at C7. The same patterns for the C7 and N8 polarizations are apparent for noncombined folate (Table IV), and for noncombined folate with the 6-31G** basis set in Table VI (same calculation as reported in ref. 23 and shown in Table I); these results also show MP2 results similar to the HF results, and GGA (B3LYP) results similar to the LDA results. The effect can also be clearly seen in Figure 5, which shows electron density changes at both the HF and LDA DFT levels of theory with the 6-31G** basis set. Note that we have undertaken a larger number of calculations than reported here, and all basis sets show this same behavior.

The differences in the polarization behavior of substrates between the HF and LDA calculations are most easily understood by considering Figure 5 in conjunction with folate residue and total numbers in Tables IV and VI. Overall, the pterin ring is much more polarized at the LDA level than at the HF level, particularly in the regions adjacent to Asp27 (N2—C2—N3), but atoms N5, C6, C7, and N8 also show marked decreases in electron density (blue isosurfaces) upon binding at the LDA level of theory when compared with the HF calculations. At the HF level, changes in density in the region of the reducible bond (N8—C7) are relatively small, with the bulk of the polarization taking place in

TABLE IV.

Per-Atom Charges, Per-Residue Charges, and Polarization for Atoms of Pterin Ring for Combined QM System of Folate and NADPH in Gas Phase and within *E. coli* DHFR (7DFR) at the HF and DFT LDA (SVWN5) Levels, Using the 6-31G* Basis Set[a] (Results in Parentheses Are for the Noncombined Folate System with 6-31G* Basis Set).

	Charges[b]				Polarization[b,c]	
	HF		LDA			
	Gas phase	Enzyme	Gas phase	Enzyme	HF	LDA
N1	−0.694	−0.750	−0.917	−0.929	−0.055	−0.012
C2	0.863	0.835	1.118	1.123	−0.028	0.005
N2	−0.898	−0.909	−1.101	−1.115	−0.012	−0.014
N3	−0.893	−0.892	−1.036	−1.023	0.002	0.013
C4	0.860	0.849	0.911	0.960	−0.011	0.049
O4	−0.652	−0.634	−0.723	−0.654	0.019	0.069
C4a	0.119	0.109	0.530	0.530	−0.010	−0.001
N5	−0.503	−0.500	−0.954	−0.910	0.004	0.043
C6	0.242 (0.246)	0.215 (0.221)	0.463 (0.306)	0.467 (0.302)	−0.027 (−0.024)[d]	0.004 (−0.004)
C7	0.013 (0.036)	0.001 (0.031)	0.072 (−0.083)	0.087 (−0.061)	−0.012 (−0.005)	0.015 (0.021)
N8	−0.494 (−0.496)	−0.511 (−0.515)	−0.855 (−0.398)	−0.826 (−0.372)	−0.017 (−0.018)	0.029 (0.027)
C8a	0.551	0.549	0.684	0.697	−0.002	0.014
H2	0.400	0.401	0.367	0.393	0.001	0.026
H2′	0.368	0.401	0.336	0.403	0.041	0.067
H3	0.398	0.549	0.351	0.540	0.151	0.189
H7	0.216	0.199	0.176	0.215	−0.017	0.039
Total PTER	−0.107 (−0.068)	−0.080 (−0.032)	−0.579 (−0.422)	−0.043 (0.051)	0.028 (0.037)[d]	0.536 (0.473)[e]
p-ABA	0.180 (0.143)	0.242 (0.202)	0.109 (−0.137)	0.267 (−0.039)	0.062 (0.059)	0.158 (0.097)
GLU	−2.095 (−2.074)	−2.190 (−2.170)	−1.992 (−1.441)	−2.307 (−2.011)	−0.095 (−0.096)	−0.316 (−0.570)
Total folate	−2.022 (−2.000)	−2.028 (−2.000)	−2.462 (−2.000)	−2.083 (−2.000)	−0.005 (0.000)	0.378 (0.000)
Total NADPH	−3.978	−3.972	−3.538	−3.917	0.005	−0.378

[a] Same system as in Table I. See Table V for analogous results for NADPH.
[b] Charges and polarizations in terms of Mulliken charges.
[c] Polarization as Δ(enzyme − gas phase).
[d] MP2 results for noncombined folate with 6-31G* basis for PTER, *p*-ABA, and GLU: 0.044, 0.077, −0.121. For C6, C7, and N8 polarizations: −0.019, −0.008, −0.017.
[e] See Table I for LDA DFT results of Bajorath et al.[20] for noncombined folate with the 6-31G** basis set.

TABLE V.

Per-Atom Charges, Per-Residue Charges, and Polarization for Atoms of Nicotinamide Ring for Combined QM System of Folate and NADPH in Gas Phase and within *E. coli* DHFR (7DFR) at HF and DFT LDA (SVWN5) Levels, Using the 6-31G* Basis Set[a] (Results in Parentheses Are for Noncombined NADPH System with 6-31G* Basis Set, Including at the MP2 Level).

	Charges[b]						Polarization[b,c]		
	HF		MP2		LDA				
	Gas phase	Enzyme	Gas phase	Enzyme	Gas phase	Enzyme	HF	MP2	LDA
N1	−0.756	−0.755			−1.004	−1.003	0.001		0.001
C6	0.174	0.110			0.198	0.162	−0.063		−0.036
C5	−0.204	−0.218			0.092	0.076	−0.014		−0.016
C7	0.751	0.765			0.796	0.806	0.015		0.010
O7	−0.694	−0.747			−0.694	−0.741	−0.053		−0.047
N7	−0.896	−0.885			−1.045	−1.029	0.010		0.016
C4	−0.261 (−0.258)	−0.294 (−0.289)	(−0.320)	(−0.348)	−0.573 (−0.393)	−0.597 (−0.424)	−0.034 (−0.031)	(−0.029)	−0.024 (−0.031)
C3	−0.328	−0.371			−0.280	−0.326	−0.043		−0.046
C2	0.149	0.133			0.260	0.247	−0.015		−0.013
H4[d]	0.163 (0.153)	0.159 (0.139)	(0.151)	(0.137)	0.320 (0.137)	0.283 (0.144)	−0.003 (−0.014)	(−0.014)	−0.037 (0.007)
H4′	0.184 (0.181)	0.263 (0.255)	(0.176)	(0.251)	0.238 (0.162)	0.330 (0.263)	0.079 (0.075)	(0.075)	0.091 (0.101)
Total NICO	−0.301 (−0.326)	−0.270 (−0.299)	(−0.263)	(−0.230)	−0.318 (−0.579)	−0.191 (−0.170)	0.031 (0.028)	(0.032)	0.127 (0.410)[e]
DIPHO	−2.491 (−2.491)	−2.594 (−2.594)	(−2.324)	(−2.429)	−2.108 (−2.089)	−2.289 (−2.251)	−0.102 (−0.103)	(−0.105)	−0.181 (−0.162)
RIB1	0.523 (0.519)	0.582 (0.578)	(0.371)	(0.431)	0.353 (0.175)	0.452 (0.294)	0.059 (0.059)	(0.060)	0.098 (0.119)
RIB2	0.875 (0.877)	0.903 (0.905)	(0.626)	(0.651)	0.838 (0.443)	0.801 (0.426)	0.028 (0.028)	(0.025)	−0.038 (−0.018)
ADPHO	−2.156 (−2.154)	−2.169 (−2.167)	(−2.027)	(−2.043)	−1.651 (−1.465)	−1.816 (−1.631)	−0.013 (−0.013)	(−0.016)	−0.165 (−0.166)
ADEN	−0.428 (−0.425)	−0.425 (−0.422)	(−0.383)	(−0.379)	−0.653 (−0.484)	−0.872 (−0.668)	0.003 (0.003)	(0.003)	−0.219 (−0.183)
Total NADPH	−3.978 (−4.000)	−3.972 (−4.000)	(−4.000)	(−4.000)	−3.538 (−4.000)	−3.917 (−4.000)	0.005 (0.000)	(0.000)	−0.378 (0.000)
Total folate	−2.022	−2.028			−2.462	−2.083	−0.005		0.378

[a] Same system as in Table I. See Table IV for analogous results for folate.
[b] Charges and polarizations in terms of Mulliken charges.
[c] Polarization as Δ(enzyme − gas phase).
[d] H4 is the active hydrogen transferred.
[e] See Table I for LDA DFT results of Bajorath et al.[21] for noncombined NADPH with the 6-31G** basis set.

TABLE VI.

Per-Atom Polarizations[a] for Atoms of Pterin Ring of Folate or Dihydrofolate within *E. coli* DHFR (7DFR) at Several Levels of Theory, Using the 6-31G Basis Set.**

	Folate[b]				Dihydrofolate			
	HF	MP2	GGA[c]	LDA	HF	MP2	GGA	LDA
N1	−0.054	−0.051	−0.038	−0.028	−0.052	−0.049	−0.040	−0.029
C2	−0.030	−0.037	−0.025	−0.019	−0.033	−0.039	−0.019	−0.009
N2	0.004	0.006	0.012	0.017	0.001	0.002	0.012	0.016
N3	−0.001	−0.002	−0.009	−0.009	−0.002	−0.003	0.001	−0.004
C4	−0.008	−0.009	0.021	0.038	−0.001	−0.002	0.011	0.022
O4	0.021	0.022	0.052	0.067	0.020	0.022	0.041	0.053
C4a	−0.007	−0.005	−0.003	0.000	−0.019	−0.017	−0.009	−0.004
N5	0.004	−0.005	0.040	0.053	0.022	0.007	0.028	0.038
C6	−0.025	−0.019	−0.010	−0.003	−0.032	−0.017	0.004	0.016
C7	−0.005	−0.008	0.012	0.021	0.020	0.015	0.001	−0.007
N8	−0.019	−0.017	0.015	0.026	−0.030	−0.031	−0.027	−0.025
C8a	−0.004	−0.006	0.003	0.011	−0.006	−0.009	0.015	0.024
H2	0.001	0.004	0.014	0.023	0.000	0.003	0.013	0.023
H2′	0.039	0.040	0.052	0.061	0.041	0.043	0.056	0.069
H3	0.139	0.150	0.172	0.187	0.140	0.152	0.165	0.187
H7	−0.018	−0.020	0.011	0.028	−0.087	−0.085	−0.055	−0.069
H7′	—	—	—	—	0.047	0.047	0.067	0.081
H8	—	—	—	—	0.008	0.008	0.018	0.025
Total PTER	0.037	0.044	0.321	0.472	0.037	0.045	0.267	0.421
p-ABA	0.060	0.078	0.102	0.097	0.059	0.077	0.102	0.105
GLU	−0.097	−0.122	−0.423	−0.570	−0.097	−0.122	−0.369	−0.526

[a] Polarizations in terms of Mulliken charges.
[b] Full results corresponding to calculation in ref. 23 (see Table I).
[c] GGA DFT method is B3LYP.

the N2—C2—N3 region. However, it is clear that the underlying reason for these changes is the large net depletion of electron density in the pterin ring (the blue polarization isosurfaces dominating) and increase in density at the glutamate end of folate (red polarization isosurfaces dominate), at the LDA level. At the HF level, however, no such dipolar shift of density from pterin to glutamate is apparent: there are red and blue isosurfaces of approximately the same size in both the pterin and glutamate residues. Note that Figure 5 was generated from a noncombined folate calculation; that is, the loss of electrons from the pterin ring, and also now from the *p*-ABA group, would be even more marked for density plots generated from combined calculations that show a net loss of electrons from folate (Tables I and IV).

For cofactor, the HF results in Table V for the combined and noncombined NADPH calculations, and the MP2 results for noncombined NADPH calculations, indicate that the charge polarization at the active carbon (C4) and for the active hydrogen (H4) are both favorable for hydride-ion transfer (i.e., slightly more negative) on binding to the enzyme. This pattern also applies to the LDA results, except for the H4 polarization for the noncombined calculation. Interestingly, for all three methods and systems, the nonactive hydrogen (H4′) becomes significantly more positive on binding to the enzyme, which reduces its potential for transfer. In the enzyme, H4′ is close to the hydroxyl oxygen of Tyr100, which provides a straightforward reason for its electron depletion on binding to the enzyme.

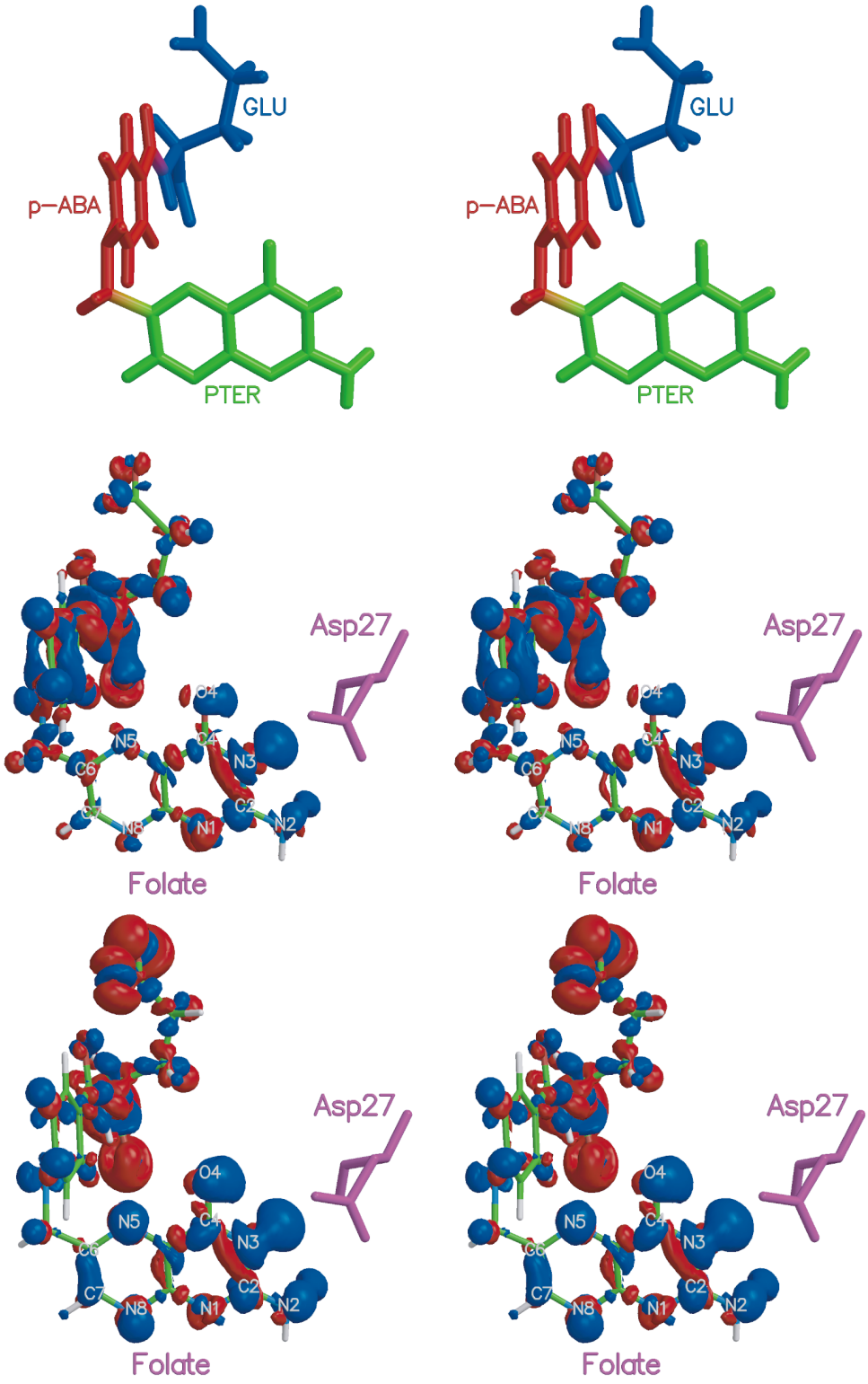

FIGURE 5. Stereoplots showing enzyme polarization isodensity surfaces for folate within *E. coli* DHFR at the HF/6-31G** (middle) and LDA/6-31G** (bottom) levels of theory. Isosurfaces are at +0.001 (red) and −0.001 (blue) electrons bohr^{-3}. Red and blue surfaces indicate regions of increased and decreased electron density on binding, respectively. The top figure shows the relative positions of the PTER, *p*-ABA, and GLU residues within folate. Figure rendered using MOLSCRIPT[24] and RASTER3D.[50] Surfaces generated from GAUSSIAN-98[51] densities using in-house code.

COMPONENTS OF POLARIZATION OF PTERIN AND NICOTINAMIDE RINGS FROM *AB INITIO* QM

It is enlightening to examine the origins of these net polarizations by consideration of the component results for the gas-phase and enzyme-embedded calculations shown in Table IV (folate) and Table V (NADPH). Very unusual behavior for these components is apparent from the LDA calculations at the folate and NADPH residue levels for both combined and noncombined calculations. The following analysis is focused at the residue level as summations of charges over groups of atoms averages out much of the arbitrariness of atomic population analysis. The atom-wise charges for the pterin and nicotinamide rings are, however, also given.

For the noncombined folate LDA calculation, as discussed previously,[23] the gas-phase result shows only −1.44 charge on the GLU residue compared with an expected formal ∼2 electrons with the charge moving mostly to the PTER residue (−0.42). As there is no formal mechanism, such as conjugation, for the pterin to acquire electrons from the glutamate group, this DFT polarization behavior appears anomalous. By contrast, the enzyme-embedded LDA result (GLU −2.01, PTER 0.05) shows the expected pattern, which is similar to the HF results; that is, both the combined and noncombined folate HF calculations show little polarization in the gas phase (GLU ∼−2.1, PTER ∼−0.1) and in the enzyme (GLU ∼−2.2, PTER −0.1). For the combined LDA gas-phase calculation, the pattern is quite different. In this case, there is still a large build-up of charge on the PTER residue (−0.58), but the GLU formal charge is not depleted (−1.99), the excess electrons being supplied by charge transfer from NADPH to give a total folate charge of −2.46. For the enzyme-embedded result, there is the same large reversal of charge build-up on the PTER residue (now only −0.04) observed for the noncombined calculation, with much of the charge moving back to NADPH (folate total charge now −2.08), but with a charge build-up on the GLU residue now observed (−2.31). There is significant depletion of electrons on the *p*-ABA residue for both combined and noncombined HF calculations and for the combined LDA calculation, with this depletion being larger in the enzyme-embedded components (∼0.25 for combined HF and LDA results). The same trend (i.e., enzyme-embedded component more positive), but with different absolute values, is apparent for the noncombined LDA results (gas phase −0.14, enzyme −0.04).

For the noncombined NADPH system (Table V), the LDA gas-phase and enzyme-embedded results show the formally dianionic residues (DIPHO and ADPHO) to be substantially less negative than the corresponding HF and MP2 results, with the ADPHO group having an electron deficit (∼−1.5 compared with ∼2.2) and the DIPHO group having fewer excess electrons (∼−2.2 compared with ∼−2.5). The LDA calculations showing the most marked polarization are for the NICO group (0.4 compared with 0.03 for HF and MP2), which has substantially more electrons in the gas phase than HF and MP2. This large polarization is coupled with substantial charge transfers to the ADPHO (−0.17), DIPHO (−0.16), and ADEN (−0.18) groups from the enzyme-embedded calculation; that is, a dipolar shift comparable with that observed for noncombined folate at the LDA level.

For the LDA combined NADPH system, the DIPHO and ADPHO groups have a slight excess (−2.11), or substantial deficit (−1.65), of charge in the gas phase. There are charge increases on both groups in the enzyme (to −2.29 and −1.82, respectively). Most of this trend can be accounted for by the substantial net transfer of electrons to folate in the gas phase (NADPH total charge −3.54), which is substantially reduced in the enzyme (NADPH total charge −3.92). In contrast to the noncombined result, the NICO group is much less charged in the gas phase (−0.32 compared with −0.58), leading to a much lower polarization (0.13 compared with 0.41). The ADEN group is more charged (−0.65 compared with −0.48 in the gas phase), but the polarization is similar to the noncombined result (−0.22 and −0.18). Both the RIB1 and RIB2 groups are substantially positive at all levels of theory, especially the RIB2 group. The gas-phase and enzyme-embedded HF results show that both the DIPHO (∼−2.6) and ADPHO (∼−2.2) groups are substantially more negative than in the LDA calculations, but there is little loss in charge to folate for either gas-phase (NADPH total charge −3.98) or enzyme-embedded (NADPH total charge −3.97) calculations. Rather, electrons have been transferred from the RIB1 and RIB2 groups to the DIPHO, ADPHO, and also NICO and ADEN groups so that there are substantial dipolar shifts within NADPH, but these are similar in both the gas-phase and enzyme-embedded calculations. Thus, as for combined folate, and in contrast to the LDA calculations, there is no large polarization of NADPH after binding to the enzyme.

TABLE VII.
Per-Atom Charges and Polarization for Atoms of Pterin Ring of Folate or Dihydrofolate within Human DHFR (1DRF) Using AM1 Mozyme Methodology.

	Folate			Dihydrofolate		
	Gas phase	Enzyme	Polarization	Gas phase	Enzyme	Polarization
N1	−0.232	−0.297	−0.065	−0.290	−0.351	−0.060
C2	0.250	0.249	−0.001	0.269	0.266	−0.003
N2	−0.373	−0.365	0.009	−0.377	−0.369	0.008
N3	−0.309	−0.331	−0.022	−0.308	−0.332	−0.024
C4	0.380	0.399	0.019	0.388	0.408	0.020
O4	−0.268	−0.307	−0.039	−0.278	−0.318	−0.041
C4a	−0.172	−0.230	−0.058	−0.242	−0.307	−0.065
N5	−0.060	−0.055	0.005	−0.062	−0.052	0.010
C6	−0.105	−0.138	−0.034	−0.110	−0.144	−0.034
C7	−0.094	−0.112	−0.018	−0.044	−0.038	0.006
N8	−0.093	−0.106	−0.013	−0.308	−0.314	−0.006
C8a	0.037	0.050	0.014	0.142	0.160	0.018
H2	0.261	0.250	−0.011	0.259	0.249	−0.010
H2′	0.221	0.283	0.062	0.222	0.285	0.062
H3	0.239	0.307	0.068	0.237	0.305	0.069
H7	0.168	0.203	0.035	0.083	0.088	0.005
H7′	—	—	—	0.076	0.080	0.005
H8	—	—	—	0.220	0.218	−0.002
PTER	−0.150	−0.200	−0.050	−0.125	−0.166	−0.041
p-ABA	−0.071	0.014	0.086	−0.093	−0.007	0.086
GLU	−1.779	−1.792	−0.013	−1.782	−1.795	−0.013
Total substrate	−2.000	−1.978	0.022	−2.000	−1.968	0.032

EFFECT OF BASIS SET SIZE

The effect on enzyme polarization from increasing the size of the basis set is small compared with the differences due to the theoretical method used (Tables I and VI). For all basis sets considered, polarization using any of the density functional methods (LDA and GGA/B3LYP in this study, and two other GGA methods in the initial work[23]) is substantially greater than the HF polarization at the same basis set. For polarizations of folate and NADPH within *E. coli* DHFR (7DFR) shown in Table I, the effect of increasing the basis set size from 3-21G to 6-31G* is minimal for both HF or LDA methods. Further increasing the size of the basis set from 6-31G* to 6-31+G* by addition of diffuse basis functions leads to an expected increase in the polarizability of both ligands, but the magnitude of the polarization is still markedly less than by the DFT methods. Unfortunately, the DFT calculation at this basis set level failed to converge, but greater polarization could be expected.

COMPARISON OF FOLATE AND DIHYDROFOLATE POLARIZATION

Keeping in mind the results of the effects of level of theory, basis set, and combined or noncombined calculation just discussed for folate, we now compare the polarizations for the pterin rings of folate and dihydrofolate to evaluate the significance of possible differences for promoting the first and second reductions shown in Figure 1. Results for the HF, MP2, LDA, and GGA levels of theory with the 6-31G** basis set for the noncombined substrates in *E. coli* DHFR (7DFR) are shown in Table VI. At the HF and MP2 levels, the polarization of dihydrofo-

TABLE VIII.
Per-Atom Charges, Per-Residue Charges, and Polarizations for Atoms of Pterin Ring of Folate within *E. coli* DHFR (7DFR) Using AM1 Mozyme Methodology, with NADPH Cofactor Present (SC) or Absent (S).[a]

	Gas phase (S)	Gas phase (SC)	Enzyme (S)	Enzyme (SC)	Polarization (S)	Polarization (SC)
N1	−0.243	−0.218	−0.328	−0.309	−0.085	−0.091
C2	0.225	0.204	0.230	0.218	0.005	0.014
N2	−0.305	−0.310	−0.258	−0.266	0.047	0.044
N3	−0.329	−0.329	−0.332	−0.335	−0.003	−0.006
C4	0.343	0.351	0.355	0.363	0.012	0.012
O4	−0.315	−0.344	−0.327	−0.355	−0.012	−0.011
C4a	−0.144	−0.132	−0.184	−0.175	−0.039	−0.043
N5	−0.010	−0.031	0.003	−0.018	0.014	0.013
C6	−0.103	−0.078	−0.144	−0.118	−0.041	−0.040
C7	−0.090	−0.080	−0.087	−0.079	0.003	0.001
N8	−0.066	−0.063	−0.094	−0.093	−0.029	−0.030
C8a	0.048	0.058	0.074	0.084	0.026	0.026
H2	0.222	0.215	0.212	0.208	−0.010	−0.007
H2′	0.205	0.186	0.230	0.216	0.025	0.030
H3	0.243	0.228	0.315	0.306	0.072	0.078
H7	0.153	0.166	0.141	0.154	−0.011	−0.012
PTER	−0.166	−0.177	−0.192	−0.198	−0.026	−0.021
p-ABA	0.049	0.083	0.114	0.141	0.065	0.058
GLU	−1.883	−1.905	−1.954	−1.967	−0.071	−0.062
Total folate	−2.000	−1.999	−2.032	−2.025	−0.032	−0.026
NICO	—	−0.208	—	−0.196	—	0.012
Total NADPH	—	−4.001	—	−3.686	—	0.315
Total folate + NADPH	—	−6.000	—	−5.711	—	0.289

[a] Complementary results for NADPH in Table IX.

late at C6 has the same (negative) sign as for folate at C7—that is, unfavorable for direct hydride-ion transfer. However, while the trend (more negative) at N8 for folate favors protonation, the trend at N5 for dihydrofolate disfavors it. At the DFT levels, the trends at both C7 of folate and C6 of dihydrofolate favor direct hydride-ion transfer; however, as discussed earlier for folate and apparent in Table VI, and also previously[22, 23] for dihydrofolate, this electron depletion arises mostly from the large (anomalous) charge depletion of the PTER residue in the enzyme. At the residue level, the polarizations for dihydrofolate are similar to those for folate at all levels, although the charge shift from the PTER to GLU residues is somewhat less exaggerated at the GGA and LDA levels. The same pattern of polarization of the pyrimidine ring near the Asp27 group is apparent for dihydrofolate and for folate (cf. Fig. 5).

EFFECT OF CHARGE-FIELD REPRESENTATION

Point charges, with values generally taken from MM force fields, are often used in the representation of an external environment within QM/MM calculations. However, as the values of the charges often differ substantially depending on the formulation of the force field, we evaluated the significance of this variable on the polarization of the DHFR-bound ligands using a number of common force fields (i.e., AMBER95, CFF91, CVFF, and ESFF). HF results with the 6-31G* basis set in Table II for the combined fo-

TABLE IX.

Per-Atom Charges, Per-Residue Charges, and Polarizations for Heavy Atoms and C4 Hydrogens of Nicotinamide Ring of NADPH within *E. coli* DHFR (7DFR) Using AM1 Mozyme Methodology, with Folate Present (SC) or Absent (C).[a]

	Gas phase (C)	Gas phase (SC)	Enzyme (C)	Enzyme (SC)	Polarization (C)	Polarization (SC)
N1	−0.222	−0.225	−0.236	−0.237	−0.014	−0.012
C6	0.060	0.055	0.025	0.022	−0.035	−0.033
C5	−0.279	−0.268	−0.259	−0.253	0.020	0.015
C7	0.334	0.334	0.350	0.350	0.016	0.016
O7	−0.430	−0.421	−0.477	−0.472	−0.047	−0.051
N7	−0.386	−0.387	−0.358	−0.359	0.028	0.028
C4	−0.025	−0.034	−0.039	−0.049	−0.014	−0.015
C3	−0.255	−0.267	−0.292	−0.305	−0.037	−0.038
C2	−0.010	0.004	−0.032	−0.028	−0.022	−0.032
H4[b]	0.067	0.069	0.068	0.070	0.001	0.001
H4′	0.087	0.091	0.121	0.125	0.034	0.034
NICO	−0.213	−0.208	−0.196	−0.196	0.017	0.012
DIPHO	−2.159	−2.157	−2.066	−2.063	0.093	0.094
RIB1	0.258	0.260	0.351	0.354	0.093	0.094
RIB2	0.386	0.382	0.431	0.428	0.045	0.046
ADPHO	−1.977	−1.979	−1.944	−1.946	0.033	0.033
ADEN	−0.296	−0.299	−0.262	−0.265	0.034	0.034
Total NADPH	−4.000	−4.001	−3.686	−3.686	0.315	0.313
PTER	—	−0.177	—	−0.198	—	−0.021
Total folate	—	−1.999	—	−2.025	—	−0.026
Total NADPH + folate	—	−6.000	—	−5.711	—	0.289

[a] Complementary results for folate are in Table VIII.
[b] H4 is the active hydrogen transferred.

late and NADPH system in *E. coli* DHFR (1RA2) show the same trends and similar absolute polarizations for all force fields. This does not mean that the electrostatic environment is insignificant, but rather that the choice of theoretical method has a substantially greater influence on the calculated polarization.

EFFECT OF CRYSTAL STRUCTURE USED

HF results with the 6-31G* basis in Table III for the two *E. coli* DHFR structures (7DFR and 1RA2) show only small differences for the polarizations of bound folate and NADPH: these differences can be regarded as indicative of the scale of the computational "noise." The analogous results for the polarization of folate substrates bound to *E. coli* and human DHFRs are also similar, with a similar atom-wise pattern for the PTER residue in the human enzyme, specifically for the N8 and C7 atoms observed (results not shown).

MODELING THE ENZYME USING MOZYME

Clearly, modeling the entire enzyme/substrate system explicitly is preferable to studying ligand polarization using a point charge, or other hybrid QM/MM model. Such calculations are now (just) possible, but only at the semiempirical QM level for a system of this size. We used the linear-scaling Mozyme methodology of Stewart,[29] implemented in the MOPAC2000[30] program, to study the DHFR

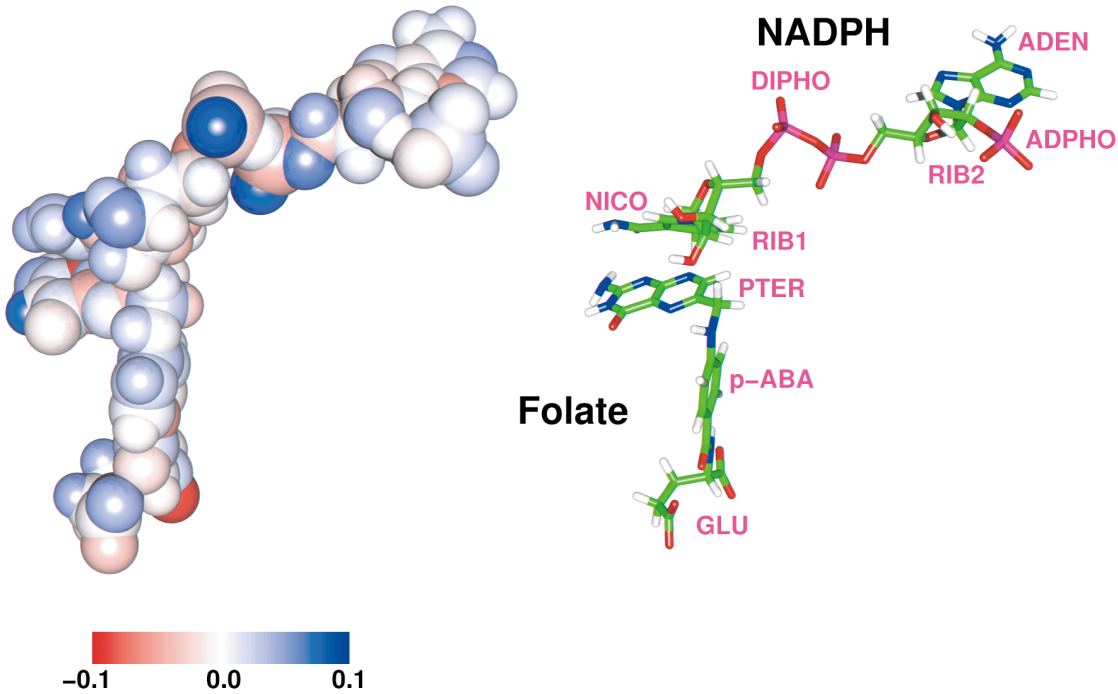

FIGURE 6. Per-atom polarization of folate and NADPH upon binding to *E. coli* DHFR (7DFR) at the AM1 level, calculated using the Mozyme methodology. The CPK model shows the polarization, whereas the ball-and-stick model (in the same orientation) shows the regions of folate and NADPH. Red and blue indicate regions of increased and decreased electron charge on binding, respectively. Figure rendered using MOLSCRIPT[24] and RASTER3D.[50]

polarization using the same fixed ligand and enzyme geometries as for the point-charge model calculations to allow for ready comparisons. Although full geometry optimization for an enzyme system of this size is feasible technically,[43] our experience in related DHFR studies is that convergence problems and the lack of efficient optimization algorithms render it computationally infeasible at present (Titmuss et al., unpublished data).

Comparisons of per-atom charges and polarizations for the pterin ring of folate and dihydrofolate in human DHFR (1DRF), and residue and molecule totals, are given in Table VII. Equivalent results for both the pterin ring of folate and nicotinamide ring of NADPH, as well as other residues, in both combined and noncombined systems within *E. coli* DHFR (7DFR) are reported in Tables VIII and IX.

Comparing the per-atom charges and polarizations for folate within human (Table VII) and *E. coli* DHFRs (Table VIII), the changes at the mechanistically important C7 and N8 atoms are relatively small. In all three sets of results, N8 becomes more negative for bound substrate and, thus, more favorable to protonation at N8. But, direct hydride-ion attack at C7 for bound substrate is either less favored (human DHFR) or unchanged (*E. coli* DHFR). For dihydrofolate within human DHFR (Table VII), the change (more negative) to C6 on binding to the enzyme does not favor direct hydride-ion attack, whereas the change at N5 (more positive) does not favor protonation either. These patterns correspond well to the findings from the HF calculations.

The general nature of the polarization of substrates, and charge transfer to NADPH and enzyme is apparent from the residue and other totals in Tables VII and VIII, and from Figure 6. For *E. coli* DHFR in both combined and noncombined calculations (Table VIII), the GLU residue is the most polarized and becomes more negative on binding, with the *p*-ABA residue more positive and the PTER residue slightly negative. This pattern for the GLU and *p*-ABA residues is the same as for the HF and MP2 calculations for folate and dihydrofolate (Tables IV and VI), but the (small) PTER polarization is reversed. For the human DHFR calculations (Table VII), however, there is little polarization of the GLU residue for either folate or dihydrofolate, whereas the *p*-ABA and PTER residues are somewhat more polarized than in the analogous (uncombined) *E. coli* DHFR results. For these human DHFR calculations, there is also negligible charge transfer to the enzyme (folate or dihydrofolate polarization

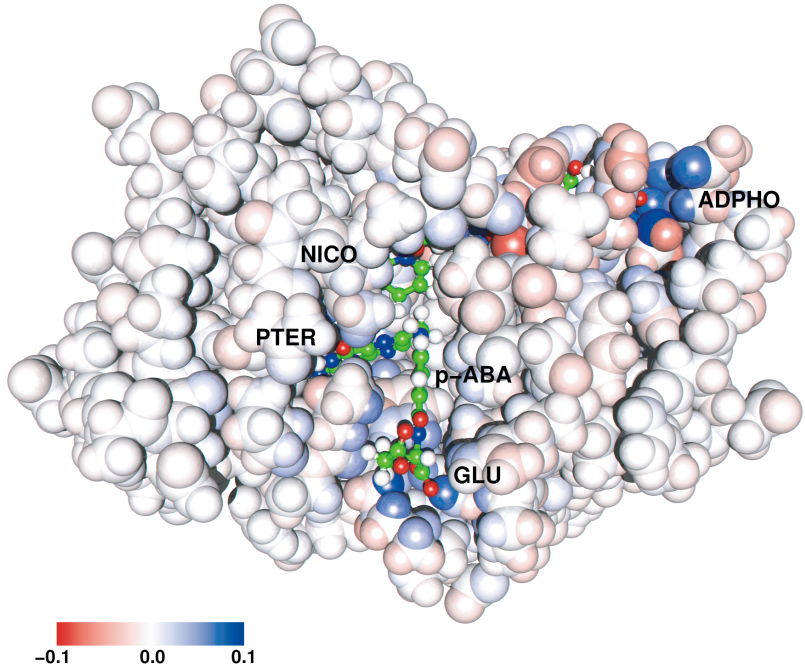

FIGURE 7. Per-atom polarization for *E. coli* DHFR (7DFR) on binding of substrate and cofactor at the AM1 level using the Mozyme methodology. The enzyme is shown in a CPK representation, with folate substrate and NADPH cofactor as ball-and-stick representation. The orientation of ligands is as shown in Figure 6. The enzyme representation is colored by polarization, with red and blue denoting a more negative and more positive charge upon binding, respectively. The dominant red regions are mostly near the formally negatively charged GLU, DIPHO, and ADPHO groups. Figure rendered using MOLSCRIPT[24] and RASTER3D.[50]

0.022 or 0.032, respectively). For the *E. coli* DHFR results, there is effectively no transfer of charge between folate and NADPH, with very little transfer to the enzyme, although in this case the folate polarization is slightly negative (∼−0.03). In terms of the residue charges within folate, either in the gas phase or in the enzyme, the Mozyme results overall show less polarization than the HF results, particularly for the *p*-ABA residue.

For the combined and noncombined NADPH calculations (Table IX), polarization at C4 (negative) would slightly facilitate hydride-ion transfer, similar to the HF results, whereas the charge on the active hydrogen H4 is unchanged. Again, as for the HF results, the nonactive H4′ becomes more positive, reducing its potential for transfer. Whereas, for both sets of results, the polarization trends (more positive) for the NICO, RIB1, RIB2, and ADEN residues parallel those for the HF results (Table V), the formally negatively charged DIPHO and ADPHO groups also both lose charge, resulting in a total loss to the enzyme of ∼0.3 electrons. Note, however, that the absolute charge on both the DIPHO and ADPHO groups is about −2, and that the polarization within NADPH either in the gas phase or in the enzyme is less by the Mozyme method than by the HF method. The regions of the enzyme that mostly gain the ∼0.3 electrons from the ligands are shown in Figure 7; these are close to the GLU, DIPHO, and ADPHO groups. The charge transfer is of very short range.

Discussion

Despite intensive study of the properties of enzyme complexes and the reaction by structural, kinetic, and biophysical methods, the chemical mechanisms for the two reduction steps catalyzed by dihydrofolate reductase remain unclear.[16] Although both steps require both proton and hydride-ion additions to the substrate, the order of these additions and the source(s) of the protons, as well as any specific differences between the two reductions, remain undefined. Although we have not specifically set out to address the question of the protonation of the pterin ring, the relatively small polarizing influence of the enzyme (at the HF and MP2 levels) does not, by itself, strongly favor the protonation of the pterin, or particularly the dihydropterin rings,

in agreement with a previous study.[19] However, this is a complex energetic issue that cannot be resolved by these calculations. We are currently undertaking high-level *ab initio* and DFT calculations to study the proton affinities of the pterin and dihydropterin rings under different models of the immediate active-site environment (Cummins and Gready, unpublished data). The pterin ring of substrates is bound in the enzyme in a large and somewhat "featureless" hydrophobic pocket, which is mostly, but not entirely, excluded from solvent access in the active ternary complex with NADPH.[16, 18] Apart from the major feature of the active site, the conserved carboxylate group (Asp in bacterial and Glu in vertebrate enzymes), the active-site environment shows little potential to polarize the reactive parts of the ligands, the pterin or dihydropterin, and nicotinamide rings. The role, especially protonation state, of this conserved carboxylate group has attracted most of the attention, but remains elusive.[16] Although experimental evidence for its ability to polarize the pyrimidine ring, including changing the tautomer or ionization state of the N3 and O4 groups of substrates bound in inactive complexes, is substantial if contradictory, such behavior might be expected from having a charged group buried in the active site and H-bonded to substrate. Even if, as sometimes proposed,[17] it were initially protonated in the active ternary complex, it is not positioned for direct transfer to either N5 of dihydrofolate or N8 of folate, although several investigators have argued for an indirect proton "hopping" from the Asp/Glu group via O4 and water molecules to N5 in dihydrofolate.[16, 17] Such a mechanism is clearly not possible for protonation of N8, and it is generally assumed that the proton for folate reduction comes from solvent.

Given this background, the series of studies by Bajorath et al.[20–22] reporting large polarizations from LDA DFT calculations of ligands bound to *E. coli* enzyme, and specifically polarizations of the N8—C7 (but not C6—N5) bond in folate and the C6—N5 bond in dihydrofolate of appropriate sign and spatial direction to facilitate the appropriate reductions, offered a new way of looking at the mechanism. These studies also reported a specific polarization of O4 in dihydrofolate, but not folate, which would support intermediate protonation of O4. However, our initial study[23] of the polarization of folate and dihydrofolate by *E. coli* DHFR using not only LDA DFT methods, but also HF, MP2, and other newer (GGA) DFT methods (the latter two classes of calculation not feasible or available to Bajorath and coworkers in 1991), did not support their conclusions. Rather, our earlier results suggested anomalous behavior from the use of DFT methods for these large anions, which was not apparent using conventional HF and MP2 *ab initio* QM methods.

Although electronic polarization or mechanical "strain" of enzyme-bound reactants in reactive complexes, in a way such as to assist the enzyme-catalyzed reaction has been much speculated on following from the original ideas of Jencks,[52] direct experimental investigation of such effects is not possible. While computational investigation is now becoming feasible, there are a great many factors that might be important, and the protocols and level of theory required to provide reliable, or at least consistent, predictions have yet to be established. Consequently, our purpose here was to evaluate the importance of several factors in calculating the polarization of substrate and cofactor ligands on binding to DHFR that were not considered in our initial study (or by Bajorath et al.), including charge transfer between ligands, and to provide a better assessment of the problem involved in using the DFT methods. We also undertook complementary calculations with a very different theoretical method, Mozyme, in which the enzyme is incorporated explicitly. We have considered the effects of: level of theory; choice of basis set; choice of charges used for representing the enzyme; choice of crystal structure coordinates, including two DHFR species with different sequence and net charge; combined versus noncombined ligand systems; and charge transfer to cofactor or enzyme. The calculations allow us to compute polarizations in specific regions of substrates and cofactor, including possible differences between folate and dihydrofolate, and to assess their magnitudes and consistency with respect to the computational variables, and hence possible significance in facilitating the hydride-ion transfer or protonation steps.

Comparing first the HF and MP2 results with the DFT results, we note that the large polarizations of both substrates and cofactor noted in our initial study, and by Bajorath et al. for LDA and GGA DFT calculations, are found also at the LDA level for the combined folate and NADPH system (i.e., all 123 atoms in the QM calculation not considered earlier). But, such gross polarizations are not observed at the HF level for either combined or noncombined systems, nor at the MP2 level for noncombined systems. Combined calculations at the MP2 level could not be performed using our current resources. However, these combined LDA DFT results now also show a large charge transfer of elec-

trons (∼0.4e) from the dianionic folate to tetraanionic NADPH molecule on binding, accompanied by a pattern of absolute charges on the component residues of the ligands in gas-phase and enzyme-embedded states, which is quite different from that of the noncombined systems. Specifically, for folate in the gas phase, the PTER and GLU groups have ∼−0.4 and ∼−0.6, and ∼−1.4 and −2.0 charges from noncombined and combined results, respectively, whereas for the enzyme-embedded state the corresponding charges are both approximately neutral for PTER and ∼−2.0 and ∼−2.3 for GLU. For NADPH there are also quite large polarizations for the LDA combined calculation results, although these are comparable with the noncombined results, except for the NICO group (∼0.13 compared with ∼0.41).

As discussed previously,[23] the origin of the apparent anomaly in the results of the DFT method seems to be from the gas-phase calculations. For folate in particular, the LDA gas-phase results show a large excess of electrons on the PTER group (∼−0.4 or ∼−0.6), which is not shown by the HF or MP2 results (∼−0.1), and which is drawn mainly from the GLU group (noncombined ∼−1.4) or NADPH (combined ∼−3.5). There are now several examples for anions in the literature indicating that DFT calculations represent their gas-phase electronic structures poorly. A recent study showed that DFT functionals poorly represent the polarizability of anions in the gas phase, a result attributed to the gas-phase anionic electron density being too diffuse at long range.[53] On inclusion of a crystalline environment (as point charges), the long-range density was compressed and physically realistic polarizabilities (and densities) were obtained.[53] These results agree with our findings for anionic ligands in the gas phase and embedded in a charge field representing the environment, where the gas-phase results show an unrealistically large dipolar character for folate and dihydrofolate, and an anomalously high charge transfer to folate from NADPH in the combined calculation, which is not shown by the enzyme-embedded calculation or the HF results. Whereas the absolute values and patterns of the residue charges for the enzyme-embedded results are more similar to the HF and MP2 results, at least for folate, the undefined nature of this "crystal" correction argues for caution also in the use of the DFT method for anions in nonisotropic "crystal" phases such as enzymes.

The calculations and analyses we have presented highlight that successful modeling of the polarization properties depends on accurate representation of both the gas-phase and enzyme-bound electronic structures of the QM region. For the systems studied here, this difficulty is compounded by the nature of the substrates and cofactor, which are formally anionic (in fact, dianionic and tetraanionic, respectively). Although there are no criteria for judging the "correctness" of calculated polarizations in any absolute sense for such limited models, except for direct comparison with experiment that is not possible for active complexes, comparisons using different theoretical methods at least allow identification of gross failures of particular methods, in this case DFT.

Considering now the HF and MP2 results, we note that the general polarization features from binding to the enzyme are represented quite well by even relatively small basis sets, especially for the ligand regions (PTER and NICO groups) involved in the reaction. The need for larger basis sets with diffuse functions arises largely from the requirements to represent the anionic character of the ligands. But, as we have shown that the anionic groups (GLU, DIPHO, ADPHO) are not only spatially distant but electronically disconnected from the reactive regions at the HF and MP2 levels, economies in future QM/MM calculations could be made by omitting the anionic parts of substrate and cofactor from the QM region or including them at a lower basis set or theory level within, for example, an ONIOM-type approach.[54] This simplification would provide greater computational scope for use of MP2 calculations to represent correlation effects. At the HF level, the polarization of ligands is quite insensitive to the choice of force-field charges, especially in comparison with the choice of basis set. The choice of charges however, could have a marked effect on other aspects of the QM/MM calculations, such as the reaction energetics.

X-ray structures are available for substrate complexes of both *E. coli*[18] and human[28] DHFRs, which have only about 30% sequence homology and with the latter having 27 extra residues[16] (many in large insertions), and for *E. coli* DHFR substrate ternary complexes in different space groups.[18, 27] This enables the effects on ligand polarization to be evaluated for species variation, including a difference in net charge of zero for human instead of −11 for *E. coli* DHFRs, and structural variability. If specific polarization of ligands by the enzyme was functionally important for the reaction mechanism, then this feature should be preserved as the enzyme evolves. HF results for the two *E. coli* DHFR structures show only small differences for the polarizations of bound folate and NADPH, which can be regarded as in-

dicative of the scale of the computational "noise." The analogous results for the polarization of folate residues bound to *E. coli* and human DHFRs are also similar, with a similar atom-wise pattern for the PTER residue in the human enzyme, specifically the N8 and C7 atoms. It would be useful to perform more refined calculations with MD-relaxed ternary complex coordinates to investigate whether there are any real, *albeit* subtle, differences between folate and dihydrofolate polarizations in different enzyme species that could arise from sequence variations near the active site, and also to evaluate whether they might be biologically significant.

For both folate and dihydrofolate at the HF and MP2 levels, the changes in density from enzyme binding in the region of the reducible bonds were small, with the bulk of the polarization taking place in the N2—C2—N3 region near the Asp27 (or Glu30) group. There is no dipolar shift of density from pterin to glutamate, nor significant charge transfer from substrate to NADPH, as found for the DFT calculations. Polarization at C7 for folate and C6 for dihydrofolate is negative; that is, does not favor hydride-ion transfer, whereas the trend at N8 for folate, but not at N5 for dihydrofolate, favors protonation. For the Mozyme results, the polarizations at the reducible bonds were also small, with the trends for C7 and N8 in folate and C6 and N5 in dihydrofolate corresponding well with the HF and MP2 results. The overall polarization of folate and dihydrofolate in the Mozyme calculations is less than for the HF and MP2 results, but there is also negligible charge transfer to NADPH, and only a small charge transfer to the enzyme ($\sim$0.03 human, $\sim-$0.03 *E. coli*).

For NADPH, both the HF (and MP2) and Mozyme results indicate that the charge polarization on binding to the enzyme at the active carbon (C4) is favorable for hydride-ion transfer (i.e., slightly more negative), with the active hydrogen (H4) also being more negative for the HF (and MP2) results but unchanged for the Mozyme results. For all methodologies, the nonactive hydrogen (H4′) becomes significantly more positive, which would reduce its potential for transfer. As for substrates, the overall polarization by Mozyme is generally less than by the HF method, with the same trends for the NICO, RIB1, RIB2, and ADEN residues (more positive), but with the formally negatively charged DIPHO and ADPHO groups now losing rather than gaining charge—an effect attributable to a net loss to the enzyme of $\sim$0.3 electrons.

Conclusions

In this work have investigated enzyme-induced polarization of DHFR substrate and cofactor ligands, and established the most important computational variables and dependence on methods. Although DFT methods appear attractive for inexpensive inclusion of correlation effects, this work, and our earlier work[23] comparing HF and MP2 results with both LDA and GGA DFT results, indicate that the large polarizations observed with the latter are largely artifactual, mostly due to their inability to represent properly these large anionic ligands in the gas phase, and thus that mechanistic inferences drawn from them are unsafe. The new Mozyme method offers great potential for a consistent and balanced treatment of ligand and enzyme, including incorporation of charge-transfer effects between ligands and enzyme, but the intrinsic limitations of semiempirical QM compared with *ab initio* QM are well-known and there are no other examples in the literature for applications except for test systems. However, it is encouraging that, while, as expected, the overall polarization of ligands is lower by the Mozyme method, the trends and mechanistic implications of the polarizations of the reducible bonds of both substrates and of the active methylene group of NADPH correspond well with those by the HF and MP2 methods. In contrast to the LDA results, these trends provide no support for facilitation of hydride-ion transfer by specific polarization of the reducible bonds of folate (N8—C7) and dihydrofolate (C6—N5). However, all methods predict polarization of C4 of NADPH, which would promote hydride-ion transfer, and also that the nonactive hydrogen would be deactivated, features that were not reported by Bajorath et al.[20–22]

Whereas analysis of enzyme-induced polarizations provides some indication of the likely effect of the enzyme on the reaction, it is important to note that this is potential only, and that the extent and manner in which the reaction proceeds will depend on the reaction pathway and the free-energy difference between the initial and final states. This is particularly the case for these heterocyclic-ring reactants where the properties of the states are properties of extended delocalized systems, and hence polarization changes in other parts of the ring will contribute to the protonation and reduction energies in a complex way not easily correlated with the observed atom-wise polarizations.[55, 56]

Although the current results are preliminary only, there are indications from the Mozyme cal-

culations for differential polarization of substrates between human and *E. coli* enzymes. Such effects might shed light on differences in folate- and dihydrofolate-reducing properties between vertebrate and bacterial DHFRs. These apparent differences appear worth pursuing with a more accurate model-building protocol and geometry optimization of the complexes by Mozyme, to allow a detailed analysis of the active-site features that might contribute to the discrimination.

Acknowledgments

Generous access to the Fujitsu VP300 under the ANUSF computing-time allocation scheme is gratefully acknowledged. We thank Dr. Andrey Bliznyuk, ANUSF, for assistance with the Mozyme calculations.

References

1. Kollman, P. A.; Merz, K. M., Jr. Acc Chem Res 1990, 23, 246–252.
2. Aqvist, J.; Warshel, A. Chem Rev 1993, 93, 2523–2544.
3. Warshel, A.; Florian, J. Proc Natl Acad Sci USA 1998, 95, 5950–5955.
4. Gao, J. Rev Comput Chem 1996, 7, 119–185.
5. Gao, J.; Thompson, M. A., Eds. Hybrid Quantum Mechanical and Molecular Mechanical Methods; American Chemical Society Symposium Series No. 712; ACS: Washington, DC, 1998.
6. Eurenius, K. P.; Chatfield, D. C.; Brooks, B. R.; Hodoscek, M. Int J Quant Chem 1996, 60, 1189–1200.
7. Lyne, P. D.; Mulholland, A. J.; Richards, W. G. J Am Chem Soc 1995, 117, 11345–11350.
8. Ranganathan, S.; Gready, J. E. J Phys Chem B 1997, 101, 5614–5618.
9. Cunningham, M. A.; Ho, L. L.; Nguyen, D. T.; Gillilan, R. E.; Bash, P. A. Biochemistry 1997, 36, 4800–4816.
10. Harrison, M. J.; Burton, N. A.; Hillier, I. H. J Am Chem Soc 1997, 119, 12285–12291.
11. Cummins, P. L.; Gready, J. E. J Comput Chem 1998, 19, 977–988.
12. van Gunsteren, W. F.; Liu, H.; Mullerplathe, F. J Mol Struct (Theochem) 1998, 432, 9–14.
13. Bentzien, J.; Muller, R. P.; Florian, J.; Warshel, A. J Phys Chem B 1998, 102, 2293–2301.
14. Stanton, R. V.; Perakyla, M.; Bakowies, D.; Kollman, P. A. J Am Chem Soc 1998, 120, 3448–3457.
15. Blakley, R. L. In: Blakley, R. L.; Benkovic, S. J., Eds. Chemistry and Biochemistry of Folates, Vol. 1; Wiley: New York, 1984; pp 191–253.
16. Blakley, R. L. Adv Enzymol 1995, 70, 23–102.
17. Brown, K. A.; Kraut, J. Faraday Disc 1992, 93, 217–224.
18. Sawaya, M. R.; Kraut, J. Biochemistry 1997, 36, 586–603.
19. Cannon, W. R.; Garrison, B. J.; Benkovic, S. J. J Am Chem Soc 1997, 119, 2386–2395.
20. Bajorath, J.; Kitson, D. H.; Fitzgerald, G.; Andzelm, J.; Kraut, J.; Hagler, A. T. Proteins 1991, 9, 217–224.
21. Bajorath, J.; Li, Z.; Fitzgerald, G.; Kitson, D. H.; Farnum, M.; Fine, R. M.; Kraut, J.; Hagler, A. T. Proteins 1991, 11, 263–270.
22. Bajorath, J.; Kraut, J.; Li, Z.; Kitson, D. H.; Hagler, A. T. Proc Natl Acad Sci USA 1991, 88, 6423–6426.
23. Greatbanks, S. P.; Gready, J. E.; Limaye, A. C.; Rendell, A. P. Proteins 1999, 37, 157–165.
24. Kraulis, P. J. J Appl Crystallogr 1991, 24, 946–950.
25. Alagona, G.; Ghio, C.; Kollman, P. A. J Mol Struct (Theochem) 1996, 371, 287–298.
26. Perakyla, M.; Kollman, P. A. J Am Chem Soc 1997, 119, 1189–1196.
27. Bystroff, C.; Oatley, S. J.; Kraut, J. Biochemistry 1990, 29, 3263–3277.
28. Oefner, C.; D'Arcy, A.; Winkler, F. K. Eur J Biochem 1988, 174, 377–385.
29. Stewart, J. J. P. Int J Quant Chem 1996, 58, 133–146.
30. Stewart, J. J. P. MOPAC 2000; Fujitsu: Tokyo, 1999.
31. Frisch, M. J.; Trucks, G. W.; Schlegel, H. B.; Gill, P. M. W.; Robb, M. A.; Cheeseman, J. R.; Keith, T. A.; Petersson, G. A.; Montgomery, J. A.; Raghavachari, K.; Al-Laham, M. A.; Zakrzewski, V. G.; Ortiz, J. V.; Foresman, J. B.; Cioslowski, J.; Stefanov, B. B.; Nanayakkara, N.; Challacombe, M.; Peng, C. Y.; Ayala, P. Y.; Chen, W.; Wong, M. W.; Andres, J. L.; Replogle, E. S.; Gomperts, R.; Martin, R. L.; Fox, D. J.; Binkley, J. S.; Defrees, D. J.; Baker, J.; Stewart, J. J. P.; Head-Gordon, M.; Gonzalez, C.; Pople, J. A. GAUSSIAN-94, Revision E.1; Gaussian: Pittsburgh, PA, 1994.
32. Ahlrichs, R.; Bar, M.; Haser, M.; Horn, H.; Kolmel, C. Chem Phys Lett 1989, 162, 165–169. TURBOMOLE is commercially available from MSI, San Diego, CA.
33. Hehre, W. J.; Radom, L.; Schleyer, P. v. R.; Pople, J. *Ab Initio* Molecular Orbital Theory; Wiley-Interscience: New York, 1986.
34. Bartolotti, L. J.; Flurchik, K. Rev Comput Chem 1996, 7, 187–216.
35. Johnson, B. G.; Gill, P. M. W.; Pople, J. A. J Chem Phys 1993, 98, 5612–5626.
36. Rienstra-Kiracofe, J. C.; Graham, D. E.; Schaefer, H. F., III Mol Phys 1998, 94, 767–787.
37. Tschumper, G. S.; Schaefer, H. F., III J Chem Phys 1997, 107, 2529–2541.
38. Curtiss, L. A.; Redfern, P. C.; Raghavachari, K.; Pople, J. A. J Chem Phys 1998, 109, 42–55.
39. Slater, J. C. The Self-Consistent Field for Molecules and Solids; McGraw-Hill: New York, 1974.
40. Vosko, S. H.; Wilk, L.; Nusair, M. Can J Phys 1980, 58, 1200–1211.
41. Lee, C.; Yang, W.; Parr, R. G. Phys Rev B 1988, 37, 785–789.
42. Becke, A. D. J Chem Phys 1993, 98, 5648–5652.
43. Stewart, J. J. P. J Mol Struct (Theochem) 1997, 401, 195–205.
44. Mulliken, R. S. J Chem Phys 1955, 23, 1833–1840.
45. INSIGHT II Program; Biosym/MSI: San Diego, CA, 1998.
46. Cornell, W. D.; Cieplak, P.; Bayly, C. I.; Gould, I. R.; Merz, K. M., Jr.; Ferguson, D. M.; Spellmeyer, D. C.; Fox, T.; Caldwell, J. W.; Kollman, P. A. J Am Chem Soc 1995, 117, 5179–5197.

47. Maple, J. R.; Hwang, M.-J.; Stockfisch, T. P.; Dinur, U.; Waldman, M.; Ewig, C. S.; Hagler, A. T. J Comput Chem 1994, 15, 162–182.
48. Dauber-Osguthorpe, P.; Roberts, V. A.; Osguthorpe, D. J.; Wolff, J.; Genest, M.; Hagler, A. T. Proteins 1988, 4, 31–47.
49. DISCOVER User Guide, Version 2.9.5; Biosym Technologies: San Diego, CA, 1994.
50. Merritt, E.A.; Bacon, D. J. Meth Enzymol 1997, 277, 505–524.
51. Frisch, M. J.; Trucks, G. W.; Schlegel, H. B.; Scuseria, G. E.; Robb, M. A.; Cheeseman, J. R.; Zakrzewski, V. G.; Montgomery, J. A., Jr.; Stratmann, R. E.; Burant, J. C.; Dapprich, S.; Millam, J. M.; Daniels, A. D.; Kudin, K. N.; Strain, M. C.; Farkas, O.; Tomasi, J.; Barone, V.; Cossi, M.; Cammi, R.; Mennucci, B.; Pomelli, C.; Adamo, C.; Clifford, S.; Ochterski, J.; Petersson, G. A.; Ayala, P. Y.; Cui, Q.; Morokuma, K.; Malick, D. K.; Rabuck, A. D.; Raghavachari, K.; Foresman, J. B.; Cioslowski, J.; Ortiz, J. V.; Stefanov, B. B.; Liu, G.; Liashenko, A.; Piskorz, P.; Komaromi, I.; Gomperts, R.; Martin, R. L.; Fox, D. J.; Keith, T.; Al-Laham, M. A.; Peng, C. Y.; Nanayakkara, A.; Gonzalez, C.; Challacombe, M.; Gill, P. M. W.; Johnson, B.; Chen, W.; Wong, M. W.; Andres,J. L.; Gonzalez, C.; Head-Gordon, M.; Replogle, E. S.; Pople, J. A. GAUSSIAN-98, Revision A.6; Gaussian: Pittsburgh, PA, 1998.
52. Jencks, W. P. Catalysis in Chemistry and Enzymology; McGraw-Hill: New York, 1969.
53. Domene, C.; Fowler, P. W.; Jemmer, P.; Madden, P. Chem Phys Lett 1999, 299, 51–56.
54. Svensson, M.; Humbel, S.; Froese, R. D. J.; Matsubara, T.; Sieber, S.; Morokuma, K. J Phys Chem 1996, 100, 19357–19363.
55. Gready, J. E. J Comput Chem 1985, 6, 377–400.
56. Gready, J. E. Biochemistry 1985, 24, 4761–4766.